

Semileptonic B Decays

Vera G. Lüth

SLAC National Laboratory Accelerator, Stanford University, USA

The following is an overview of the measurements of the CKM matrix elements $|V_{cb}|$ and $|V_{ub}|$ that are based on detailed studies of semileptonic B decays by the BABAR and Belle Collaborations and major advances in QCD calculations. In addition, a new and improved measurement of the ratios $\mathcal{R}(D^{(*)}) = \mathcal{B}(\bar{B} \rightarrow D^{(*)}\tau^-\bar{\nu}_\tau)/\mathcal{B}(\bar{B} \rightarrow D^{(*)}\ell^-\bar{\nu}_\ell)$ is presented. Here $D^{(*)}$ refers to a D or a D^* meson and ℓ is either e or μ . The results, $\mathcal{R}(D) = 0.440 \pm 0.058 \pm 0.042$ and $\mathcal{R}(D^*) = 0.332 \pm 0.024 \pm 0.018$, exceed the Standard Model expectations by 2.0σ and 2.7σ , respectively. Taken together, they disagree with these expectations at the 3.4σ level. The excess of events cannot be explained by a charged Higgs boson in the type II two-Higgs-doublet model.

I. INTRODUCTION

Over the past decade, the vast samples of B mesons recorded at the B Factories at KEK and SLAC have allowed detailed studies of semileptonic B decays. In the Standard Model (SM), these decays proceed via first-order weak interaction and are mediated by the W boson. Decays involving electrons and muons are expected to be free of non-SM contributions and are therefore well suited for the determination of the Cabibbo-Kobayashi-Maskawa (CKM) matrix elements $|V_{cb}|$ and $|V_{ub}|$. They are fundamental parameters of the SM and have to be determined experimentally. Decays involving the higher mass τ lepton provide additional information on SM processes. They are also sensitive to non-SM contributions, for instance, from the exchange of a charged Higgs boson.

This presentation will combine a summary of the current status of the measurements of the CKM matrix elements $|V_{cb}|$ and $|V_{ub}|$ from the Belle and BABAR experiments with the first report on the observation by BABAR of an excess of events beyond the SM expectations in $\bar{B} \rightarrow D^{(*)}\tau^-\bar{\nu}_\tau$ decays [1]. Here $D^{(*)}$ refers to the ground state charm mesons, D and D^* .

II. $|V_{cb}|$ AND $|V_{ub}|$

There are two experimental methods to determine $|V_{cb}|$ and $|V_{ub}|$. The first is based on the study of exclusive semileptonic B decays in which the hadron is a D , D^* , D^{**} , π , or ρ meson. The second is based on inclusive decays of the form $B \rightarrow X\ell\nu$, where X refers to either X_c or X_u , that is, to any allowed hadronic final state with charm or without charm, respectively. To extract $|V_{cb}|$ or $|V_{ub}|$ from the measured partial decay rates, both approaches depend on calculations of hadronic contributions to the matrix element. Since the two methods rely on different experimental techniques and involve different theoretical approximations, they result in largely independent measurements of $|V_{cb}|$ and $|V_{ub}|$.

The tables summarizing the results from the B Fac-

tories are taken from a recent report by the Belle and BABAR Collaborations [2]. They include updates of input parameter values and reflect the latest understanding of the theoretical uncertainties. The averages account for correlations among the various measurements. In particular, all theoretical uncertainties are considered to be correlated, as are the uncertainties on the modeling of $B \rightarrow X_c\ell\nu$ and $B \rightarrow X_u\ell\nu$ decays. Experimental uncertainties due to reconstruction efficiencies are fully correlated for measurements from the same experiment, and uncorrelated for different experiments. Statistical correlations are also taken into account, whenever available. The averaging procedure was developed by the Heavy Flavor Averaging Group (HFAG) [3].

A. $|V_{cb}|$ from $\bar{B} \rightarrow D^{(*)}\ell^-\bar{\nu}_\ell$ Decays

The "exclusive" determination of $|V_{cb}|$ relies on studies of $\bar{B} \rightarrow D\ell^-\bar{\nu}_\ell$ and $\bar{B} \rightarrow D^*\ell^-\bar{\nu}_\ell$ decays, where $\ell = e, \mu$. The differential rate for the decay $B \rightarrow D\ell\nu$ can be written as

$$\frac{d\Gamma(B \rightarrow D\ell\nu)}{dw} = \frac{G_F^2}{48\pi^3} |V_{cb}|^2 \mathcal{K}_D(w) \eta_{EW}^2 \mathcal{G}^2(w), \quad (1)$$

where $\mathcal{K}_D(w)$ is a known phase-space factor and $\eta_{EW} = 1.0066$ refers to the one-loop electroweak correction [4] defined relative to G_F from muon decay. In the limit of small lepton mass m_ℓ , $\mathcal{G}(w)$ represents a single vector form factor that depends on the ratio of meson masses $r = m_D/m_B$ and $w = v_B \cdot v_D$, the product of the four-velocities of the D and the B mesons. w is related to the four-momentum transfer $q^2 = (P_B - P_D)^2 = (P_\ell + P_\nu)^2$, namely $w = (m_B^2 + m_D^2 - q^2)/(2m_B m_D) = E_D/m_D$. The values of w are limited by kinematics, $1 \leq w_D \leq 1.59$.

The same ansatz for the differential rate also holds for $B \rightarrow D^*\ell\nu$ decays, except that the phase-space factor $\mathcal{K}_{D^*}(w)$ and w differ numerically. The form factor $\mathcal{G}(w)$ is replaced by $\mathcal{F}(w, \theta_\ell, \theta_V, \chi)$, which depends also on three angles, θ_ℓ and θ_V , the helicity angles of the lepton and the D^* , and χ is the angle between the

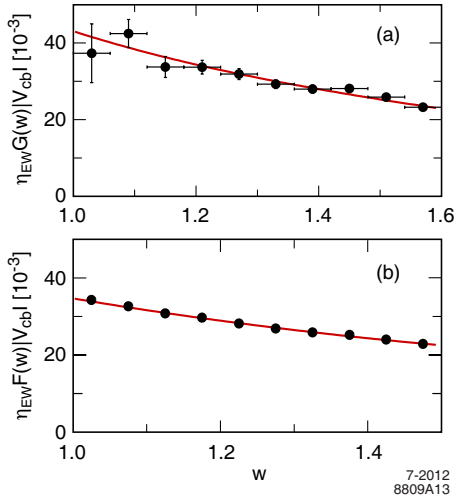


FIG. 1: *BABAR* measurements, corrected for the reconstruction efficiency, of the w dependence of the form factors, with fit results superimposed (solid line): (a) $\eta_{EW} \mathcal{G}(w) |V_{cb}|$ for $B \rightarrow D\ell\nu$ decays from tagged events [6], and for comparison (b) $\eta_{EW} \mathcal{F}(w) |V_{cb}|$ for $B \rightarrow D^*\ell\nu$ decays from untagged events [7].

decay planes of the D^* and the W . $\mathcal{F}(w, \theta_\ell, \theta_V, \chi)$ contains a combination of three form factors (one vector and two axial vectors) related to the three helicity states of the charm meson. The axial vector form factor $A_1(w)$ dominates as $w \rightarrow 1$, and therefore the decay rate is usually expressed in terms of the ratios $R_1(w) = V(w)/A_1(w)$ and $R_2(w) = A_2(w)/A_1(w)$.

In the limit of infinite b - and c -quark masses, heavy quark symmetry predicts a universal form factor $\mathcal{F}(w)$ with a normalization at zero-recoil, $\mathcal{F}(w = 1) = \mathcal{G}(w = 1)$ and a dependence on w which, with constraints from analyticity and unitarity, can be expressed in terms of a single parameter ρ_D^2 or $\rho_{D^*}^2$ [5].

The principal uncertainties for the determination of $|V_{cb}|$ stem from the form factors, both their shape and normalization. The form factor parameters are determined from fits to the differential decay rates. For $\bar{B} \rightarrow D\ell^-\bar{\nu}_\ell$ decays, $|V_{cb}| \mathcal{G}(1)$ and the slope ρ_D^2 can be extracted from $\Gamma(w)$ distribution. For $\bar{B} \rightarrow D^*\ell^-\bar{\nu}_\ell$ decays, $|V_{cb}| \mathcal{F}(1)$, the slope $\rho_{D^*}^2$, $R_1(w = 1)$, and $R_2(w = 1)$ are determined from fits to the decay distribution $\Gamma(w, \theta_\ell, \theta_V, \chi)$. As an example, Figure 1 shows the extraction of the form factor slope and normalization from the efficiency-corrected decay rates for $\bar{B} \rightarrow D\ell^-\bar{\nu}_\ell$ and $\bar{B} \rightarrow D^*\ell^-\bar{\nu}_\ell$ decays for two *BABAR* analyses.

The results of recent form factor measurements for $\bar{B} \rightarrow D\ell^-\bar{\nu}_\ell$ and $\bar{B} \rightarrow D^*\ell^-\bar{\nu}_\ell$ decays from Belle and *BABAR* are listed in Table I. The branching fractions quoted for B^0 are based on B^0 and B^+ measurements, combined under the assumptions that isospin relations hold. The branching ratios are calculated using these form factor parameters, taking into account correlated

systematic uncertainties. The errors are dominated by the uncertainties in the detector performance.

For $\bar{B} \rightarrow D^*\ell^-\bar{\nu}_\ell$ decays, only two of the four measurements exploit the angular dependence of the form factor $\mathcal{F}(w, \theta_\ell, \theta_V, \chi)$. The most precise measurement based on the full Belle data set [8] relies on a fit to the 1-dimensional distributions of the four variables. *BABAR* [7] enhances the sensitivity to $R_1(1)$ and $R_2(1)$ and also $|V_{cb}|$ by combining the results with a fit to the four-dimensional decay rate $\Gamma(w, \theta_\ell, \theta_V, \chi)$ [9]. The results from the two experiments agree well. The average values $R_1(1) = 1.40 \pm 0.03 \pm 0.01$ and $R_2(1) = 0.86 \pm 0.02 \pm 0.01$, have a precision of 3%, and are used as input to measurements that are limited to the w dependence of the decay rate.

A precise determination of $|V_{cb}|$ requires corrections to $\mathcal{G}(1)$ and $\mathcal{F}(1)$ for finite quark masses and non-perturbative effects. Table II summarizes the latest results from lattice QCD (LQCD), heavy quark sum rules (HQSR), and HQE calculation. The LQCD predictions for the two decay modes are about 5% higher than the results from the other two QCD calculations.

While the results for the two decay modes agree well, $|V_{cb}|$ measured in $B \rightarrow D^*\ell\nu$ decays is more precise and will be considered as the main result. The differences in the values for $|V_{cb}|$ underline the fact that the principal uncertainties stem from the form factor normalization.

B. $|V_{cb}|$ from Inclusive $B \rightarrow X_c\ell\nu$ Decays

At the parton level, the inclusive decay rate for $b \rightarrow c\ell\nu$ can be calculated accurately: It is proportional to $|V_{cb}|^2$ and depends on the quark masses m_b and m_c . To extract $|V_{cb}|$ from the measured B meson decay rate, the parton-level calculations have to be corrected for effects of strong interactions. These corrections are suppressed by powers of α_s and Λ_{QCD}/m_b (Λ_{QCD} refers to the perturbative QCD scale). Thus, the decay rate for inclusive semileptonic B decays can be expressed in terms of a Heavy Quark Expansion (HQE) in inverse powers of the b -quark mass and with a limited number of non-perturbative parameters. Due to confinement and non-perturbative effects, HQEs rely on the definition of the quark masses, which depends on the coupling to the SM Lagrangian.

Calculations of the decay rates for $B \rightarrow X_c\ell\nu$ are available in the $1S$ mass scheme [19, 20] which is derived from a perturbative expression for the mass of the $Y(1S)$ state, and the kinetic mass scheme [21, 22] which is derived from heavy quark sum rules and enters the non-relativistic expression for the kinetic energy of the b quark inside the B meson. In the following, we rely on calculations in the kinetic scheme for which the total decay rate for $B \rightarrow X_c\ell\nu$ can be

TABLE I: Summary of the B Factory results for the $\bar{B} \rightarrow D\ell^-\bar{\nu}_\ell$ and $\bar{B} \rightarrow D^*\ell^-\bar{\nu}_\ell$ form factor parameters $\eta_{EW}\mathcal{G}(1)|V_{cb}|$, $\eta_{EW}\mathcal{F}(1)|V_{cb}|$, ρ_D^2 and $\rho_{D^*}^2$, and the branching fractions. The measurements have been rescaled to the end of year 2011 values of the common input parameters [3, 10]. The stated errors correspond to the statistical and systematic uncertainties.

$\bar{B} \rightarrow D\ell^-\bar{\nu}_\ell$	$\eta_{EW}\mathcal{G}(1) V_{cb} $ (10^{-3})	ρ_D^2	$\mathcal{B}(B^0 \rightarrow D^-\ell^+\nu)$ (%)
Belle [11]	$40.8 \pm 4.4 \pm 5.0$	$1.12 \pm 0.22 \pm 0.14$	$2.07 \pm 0.12 \pm 0.52$
BABAR $DXl\nu$ [12]	$43.4 \pm 0.8 \pm 2.1$	$1.20 \pm 0.04 \pm 0.06$	$2.18 \pm 0.03 \pm 0.13$
BABAR tagged [6]	$42.5 \pm 1.9 \pm 1.1$	$1.18 \pm 0.09 \pm 0.05$	$2.12 \pm 0.10 \pm 0.06$
Average	$42.7 \pm 0.7 \pm 1.5$	$1.19 \pm 0.04 \pm 0.04$	$2.14 \pm 0.03 \pm 0.10$

$\bar{B} \rightarrow D^*\ell^-\bar{\nu}_\ell$	$\eta_{EW}\mathcal{F}(1) V_{cb} $ (10^{-3})	$\rho_{D^*}^2$	$\mathcal{B}(B^0 \rightarrow D^{*-}\ell^+\nu)$ (%)
BABAR $D^{*-}\ell^+\nu$ [7]	$34.1 \pm 0.3 \pm 1.0$	$1.18 \pm 0.05 \pm 0.03$	$4.58 \pm 0.04 \pm 0.25$
BABAR $\bar{D}^{*0}e^+\nu$ [13]	$35.1 \pm 0.6 \pm 1.3$	$1.12 \pm 0.06 \pm 0.06$	$4.95 \pm 0.07 \pm 0.34$
BABAR $DXl\nu$ [12]	$35.8 \pm 0.2 \pm 1.1$	$1.19 \pm 0.02 \pm 0.06$	$4.96 \pm 0.02 \pm 0.20$
Belle [8]	$34.7 \pm 0.2 \pm 1.0$	$1.21 \pm 0.03 \pm 0.01$	$4.59 \pm 0.03 \pm 0.26$
Average	$35.5 \pm 0.1 \pm 0.5$	$1.20 \pm 0.02 \pm 0.02$	$4.83 \pm 0.01 \pm 0.12$

TABLE II: Normalization of the form factors for $\bar{B} \rightarrow D\ell^-\bar{\nu}_\ell$ and $\bar{B} \rightarrow D^*\ell^-\bar{\nu}_\ell$ decays and the resulting values of $|V_{cb}|$ based on different QCD calculations.

$\bar{B} \rightarrow D\ell^-\bar{\nu}_\ell$		
Calculation	$\eta_{EW}\mathcal{G}(1)$	$ V_{cb} $ (10^{-3})
LQCD [14]	$1.081 \pm 0.018 \pm 0.016$	$39.46 \pm 1.54 \pm 0.88$
HQE [15]	1.047 ± 0.020	$40.79 \pm 1.58 \pm 0.78$

$\bar{B} \rightarrow D^*\ell^-\bar{\nu}_\ell$		
Calculation	$\eta_{EW}\mathcal{F}(1)$	$ V_{cb} $ (10^{-3})
LQCD [16, 17]	$0.908 \pm 0.005 \pm 0.016$	$39.04 \pm 0.55 \pm 0.73$
HQSR [18]	0.865 ± 0.020	$40.93 \pm 0.58 \pm 0.95$

expressed to $\mathcal{O}(1/m_b^3)$ in a simplified way as

$$\Gamma_{cl\nu} \cong \frac{G_F^2 m_b^5}{192\pi^3} |V_{cb}|^2 (1 + A_{ew}) A_{pert}(r, \mu) \times \left[z_0(r) + z_2(r) \left(\frac{\mu_\pi^2}{m_b^2}, \frac{\mu_G^2}{m_b^2} \right) + z_3(r) \left(\frac{\rho_D^3}{m_b^3}, \frac{\rho_{LS}^3}{m_b^3} \right) \right]. \quad (2)$$

A more detailed ansatz can be found in the literature [22]. The dependence on the charm quark mass m_c is contained in the ratio $r = m_c/m_b$ which enters the phase space factors $z_i(r)$. The most relevant scale for $b \rightarrow c$ transitions is the energy release $m_b - m_c$. The electroweak corrections are estimated to be $1 + A_{ew} \approx [1 + \alpha/\pi \ln(M_Z/m_b)]^2 \approx 1.014$ and the perturbative contributions are $A_{pert} \approx 0.91 \pm 0.01$. The leading non-perturbative contributions arise at $\mathcal{O}(1/m_b^2)$ and are parameterized in terms of $\mu_\pi^2(\mu)$ and $\mu_G^2(\mu)$, the expectation values of the kinetic and chro-

momagnetic dimension-five operators. At $\mathcal{O}(1/m_b^3)$, two additional parameters enter, $\rho_D^3(\mu)$ and $\rho_{LS}^3(\mu)$, the expectation values of the Darwin and spin-orbital (LS) dimension-six operators. These parameters, as well as the quark masses m_b and m_c , depend on the renormalization scale μ which separates short-distance from long-distance QCD effects. For the kinetic scheme the chosen value is $\mu = 1$ GeV [23].

Similar HQEs can be derived for moments of inclusive $B \rightarrow X_c \ell \nu$ distributions; they also depend on α_s , m_b and m_c and the same perturbative parameters. The leading terms are known to $\mathcal{O}(\alpha_s)$ and $\mathcal{O}(\alpha_s^2 \beta_0)$ (with $\beta_0 = (33 - 2n_f)/3$). Non-perturbative terms are included to $\mathcal{O}(1/m_b^3)$, and corrections to $\mathcal{O}(\alpha_s^2)$ have recently been implemented.

Moment measurements are available from $B \rightarrow X_c \ell \nu$ decays for the lepton energy spectrum $\langle E_\ell^n \rangle$ with $n = 1, 2, 3$, the hadronic mass distribution, $\langle M_X^{2n} \rangle$ with $n = 1, 2, 3$. These moments and the inclusive semileptonic decay rate $\Delta\mathcal{B}$ are measured for different values of the minimum lepton energy E_ℓ^{min} in the range of 0.6 – 1.5 GeV.

The HFAG has developed a fit procedure based on the full $\mathcal{O}(\alpha_s^2)$ calculations of the moments in the kinetic scheme [24, 25]. This fit combines moment measurements from the B Factories and determines $|V_{cb}|$, the b -quark mass m_b , and four higher order parameters in the OPE description of semileptonic decays. The only external input is the average B^0 and B^+ lifetime, (1.582 ± 0.007) ps [10].

Figure 2 shows the comparison of fitted HQE predictions in the kinetic scheme to some of the moments measured by the Belle Collaboration [26] as a function of the minimum lepton energy. Since the moments are derived from the same distribution, in particular those which differ only by the minimum lepton energy,

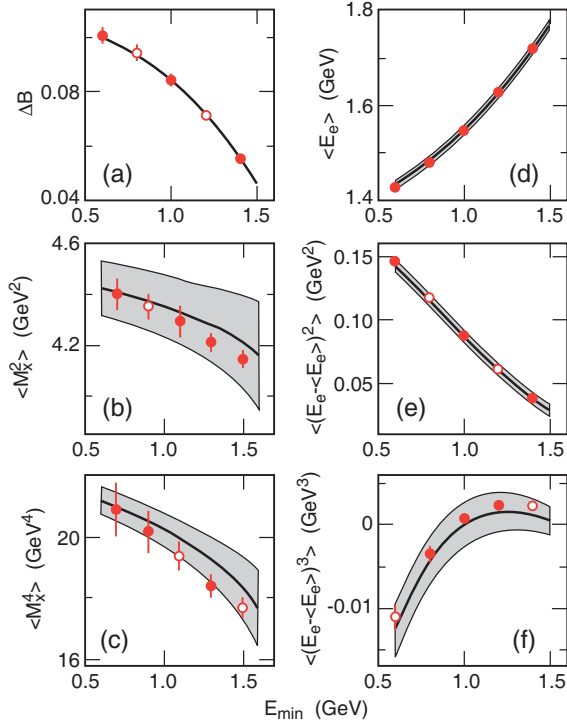


FIG. 2: Comparison of the measured moments and the fit to the HQE predictions (kinetic scheme) by the Belle Collaboration [26] as a function of the minimum lepton or photon energy: (a) branching fraction ΔB , (b,c) hadron mass (M_X), (d,e,f) and electron energy (E_e). The vertical bars represent the experimental uncertainties and the shaded bands show the theoretical uncertainties. Filled (open) circles mark data used (unused) in the fit.

are highly correlated, only about half of the measured data points are included in the fit. Similar fits have been performed by the BABAR collaboration, including also some mixed moments of different distributions, e.g., a combination of the hadronic mass and lepton energy [27].

The fit to selected 44 moments measured by Belle and BABAR has a $\chi^2/NDF = 23.2/37$, an indication that the experimental and theoretical uncertainties and estimated correlations among moments are not fully understood. Correlations between the fitted parameters are generally small.

To enhance the precision on m_b , a precise constraint on the c -quark mass $m_c(3 \text{ GeV}) = 0.998 \pm 0.029 \text{ GeV}$, was introduced, derived from low-energy sum rules [28], one of several precise calculations of quark masses [29, 30]. Fits in the kinetic scheme to the Belle and BABAR moments result in

$$\begin{aligned} |V_{cb}|_{\text{incl}} &= (42.01 \pm 0.47_{\text{fit}} \pm 0.59_{\text{th}}) \times 10^{-3}, \\ m_b^{\text{kin}}(1 \text{ GeV}) &= (4.551 \pm 0.025_{\text{fit}}) \text{ GeV}, \\ \mu_\pi^{2\text{kin}}(1 \text{ GeV}) &= (0.499 \pm 0.044_{\text{fit}}) \text{ GeV}^2. \end{aligned} \quad (3)$$

The first error represents the combined experimen-

tal and theoretical uncertainty of the fit, and the additional error on $|V_{cb}|$ reflects the estimated uncertainty of 1.4% for the expansion for the decay rate. The fitted semileptonic branching fraction is $\mathcal{B}(B \rightarrow X_c \ell \nu) = (10.51 \pm 0.13)\%$. The result on $|V_{cb}|$ cited here agrees very well with the result of a fit to the same moments based on the 1S mass scheme [2].

C. $|V_{ub}|$ from $B \rightarrow \pi \ell \nu$ Decays

For the determination of $|V_{ub}|$ from exclusive charmless decays, the most promising decays, both experimentally and theoretically, is $\bar{B} \rightarrow \pi \ell^- \bar{\nu}_\ell$. Branching fractions for decays involving the pseudoscalar mesons η and η' and the vector mesons ρ and ω have been measured, albeit with considerable uncertainties. Thus, they currently provide only limited information on form factors and therefore on $|V_{ub}|$.

As for $\bar{B} \rightarrow D \ell^- \bar{\nu}_\ell$ decays, the differential decay rate for decays to low-mass charged leptons can be written as

$$\frac{d\Gamma(B^0 \rightarrow \pi^- \ell^+ \nu)}{dq^2} = \frac{G_F^2}{24\pi^3} |p_\pi|^3 |V_{ub}|^2 |f_+(q^2)|^2. \quad (4)$$

Here $f_+(q^2)$ is the only form factor affecting the rate, because in the limit of small lepton masses m_ℓ , the term proportional to the second form factor $f_0(q^2)$ can be neglected [31]. Since the rate depends on the third power of p_π , the pion momentum in the B meson rest frame, it is suppressed at high q^2 .

Among several parameterizations of the form factors, a model-independent approach based on the general properties of analyticity, unitarity and crossing-symmetry is preferred [32, 33]. The stringent constraints on the form factor are expressed in the form of a rapidly converging series in the variable $z(q^2, q_0^2) = (\sqrt{m_+^2 - q^2} - \sqrt{m_+^2 - q_0^2}) / (m_+ - m_-)$, with $m_\pm = m_B \pm m_\pi$. The simplest functional form by Bourreley, Caprini, and Lellouch (BCL) [34] is

$$f_+(q^2) = \frac{1}{1 - q^2/m_{B^*}^2} \sum_{k=0}^K b_k(q_0^2) z(q^2, q_0^2)^k. \quad (5)$$

Here q_0^2 is a free parameter, chosen to optimize the convergence.

The principal goal of the studies of $\bar{B} \rightarrow \pi \ell^- \bar{\nu}_\ell$ decays is a precise measurement of the branching fraction and the determination of the q^2 dependence of the $B \rightarrow \pi$ form factor. The main experimental challenge is the reduction of the abundant background from continuum events and from $B \rightarrow X_c \ell \nu$ decays. Also the isolation of the $B \rightarrow \pi \ell \nu$ decays from the other $B \rightarrow X_u \ell \nu$ decays, where X_u is a charmless hadronic final state, is difficult due to very similar decay kinematics.

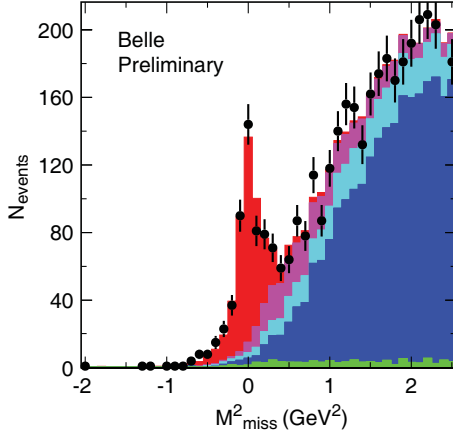


FIG. 3: Missing mass squared distribution from a tagged samples of $B^0 \rightarrow \pi^- \ell^+ \nu$ decays by the Belle Collaboration [38].

Three analyses have been performed based on untagged event samples, two by the *BABAR* [35, 36] and one by the Belle [37] Collaboration. The measured branching fractions show excellent agreements, the average, taking into account correlations, $\mathcal{B}(B^0 \rightarrow \pi^- \ell^+ \nu) = (1.44 \pm 0.03 \pm 0.05)^{-4}$, is dominated by systematic uncertainties, primarily related to the reconstruction of the missing neutrino derived from the missing energy and momentum in the event, and the backgrounds from continuum events at low q^2 and from $B \rightarrow X_u \ell \nu$ decays at high q^2 .

A few months ago the Belle collaboration [38] presented first results on exclusive charmless decays involving the pseudoscalar mesons π^+ , π^0 , η , and η' and the vector mesons, ρ^+ , ρ^0 , and ω . This analysis is based on the full data sample and benefits from a highly efficient selection of events tagged by the hadronic decay of one of the B mesons in the event. Figure 3 shows the missing mass distribution for a selected $B^0 \rightarrow \pi^- \ell^+ \nu$ sample with a purity of about 65%. From a fit to this distribution, a signal of 468 ± 28 $B^0 \rightarrow \pi^- \ell^+ \nu$ decays has been extracted. Preliminary measurements of the $d\Gamma/dq^2$ distributions and branching fractions are fully consistent with the untagged measurements (see Table III). While the statistical uncertainties are larger than for the untagged analyses, the systematic uncertainties are much reduced due to the kinematic reconstruction of the full event.

Currently, two principal methods are used to extract $|V_{ub}|$ from the measured differential decay rates. The more conventional method relates the measured partial branching fractions to $\Delta\zeta(q_{min}^2, q_{max}^2) = \Delta\Gamma_{theory}/|V_{ub}|^2$, which is derived from QCD calculations integrated over specific q^2 ranges, and

$$|V_{ub}|^2 = \Delta\mathcal{B}(q_{min}^2, q_{max}^2)/\Delta\zeta(q_{min}^2, q_{max}^2)/\tau_0, \quad (6)$$

where τ_0 is the B^0 lifetime. Table III lists the average

partial branching fractions, the values of $\Delta\zeta$, and the $|V_{ub}|$ results relying on light cone sum rules (LCSR), and two sets of LQCD calculations.

More recently, $|V_{ub}|$ has been determined from a simultaneous fit to unquenched LQCD calculations [39] and the measured q^2 spectrum. The BCL parameterization is used as parameterization for $f_+(q^2)$ over the whole q^2 range to minimize the form factor model dependence. This method makes optimum use of the measured shape of the whole q^2 spectrum and normalization from LQCD which results in a reduced uncertainty on $|V_{ub}|$.

Figure 4 shows the combined fit to the FNAL/MILC lattice calculations and the data from the three untagged measurements. To avoid high correlations, only four of the twelve FNAL/MILC points have been included in the fit. This reduction of the theoretical input does not change the $|V_{ub}|$ result but leads to a better agreement of the fitted curve with the lattice points. The χ^2 probability of the fit is 2.2% ($\chi^2/ndf = 58.9/31$). The fit results for the parameters in the BCL parameterization are $b_1/b_0 = -0.82 \pm 0.20$ and $b_2/b_0 = -1.63 \pm 0.62$, and a value of $f_+(0)|V_{ub}| = 0.945 \pm 0.028$ is obtained, which translates to $f_+(0) = 0.29 \pm 0.03$, in good agreement with the LCSR result, $f_+(0) = 0.28 \pm 0.02$. The $|V_{ub}|$ values obtained from fits to the individual untagged measurements agree with each other within about one standard deviation. The total uncertainty on $|V_{ub}|$ is about 9%; 3% from the branching fraction measurement, 4% from the shape of the q^2 spectrum determined with data, and 8% from the form-factor normalization obtained from LQCD.

Table III summarizes various measurements of $|V_{ub}|$, based on different form factor normalizations. In addition to the three untagged analysis, it also lists the preliminary results by Belle using the new tagging algorithm. All these results are fully consistent within the stated uncertainties.

D. $|V_{ub}|$ from Inclusive $B \rightarrow X_u \ell \nu$ Decays

The total inclusive rate for $B \rightarrow X_u \ell \nu$ decays can be expressed in terms of an OPE which has a similar structure as the one for $B \rightarrow X_c \ell \nu$ decays, with nonperturbative corrections occurring at $O(1/m_b^2)$ and higher. Unfortunately, experimenters usually restrict the phase space to reduce the large background from Cabibbo-favored $B \rightarrow X_c \ell \nu$ decays, and these restrictions spoil the HQE convergence. Perturbative and non-perturbative corrections are drastically enhanced and the rate becomes sensitive to the Fermi motion of the b quark inside the B meson, introducing terms that are not suppressed by powers of $1/m_b$. In practice, non-perturbative shape functions (SF) are introduced, which to leading order in $1/m_b$ should be similar for $b \rightarrow u$ and $b \rightarrow s$ transitions. The form of the

TABLE III: Overview of $|V_{ub}|$ measurements based on $B \rightarrow \pi \ell \nu$ decays (for 3 untagged and 1 tagged samples) for various q^2 regions and form factor calculations: LCSR [40], HPQCD [41], FNAL/MILC [39]. The quoted errors on $|V_{ub}|$ are due to experimental uncertainties and theoretical uncertainties on $\Delta\zeta$. The last column shows the $|V_{ub}|$ results of the simultaneous fits to data and the FNAL/MILC prediction. Here the stated error represents the combined experimental and theoretical uncertainty.

	LCSR	HPQCD	FNAL/MILC	FNAL/MILC fit
$\Delta\zeta$ (ps^{-1})	$4.59^{+1.00}_{-0.85}$	2.02 ± 0.55	$2.21^{+0.47}_{-0.42}$	$2.21^{+0.47}_{-0.42}$
q^2 range (GeV^2)	0 – 12	16 – 26.4	16 – 26.4	16 – 26.4
Experiment	$ V_{ub} $ (10^{-3})			
BABAR (6 bins) [35]	$3.54 \pm 0.12^{+0.38}_{-0.33}$	$3.22 \pm 0.15^{+0.55}_{-0.37}$	$3.08 \pm 0.14^{+0.34}_{-0.28}$	2.98 ± 0.31
BABAR (12 bins) [36]	$3.46 \pm 0.10^{+0.37}_{-0.32}$	$3.26 \pm 0.19^{+0.56}_{-0.37}$	$3.12 \pm 0.18^{+0.35}_{-0.29}$	3.22 ± 0.31
Belle [37]	$3.44 \pm 0.10^{+0.37}_{-0.32}$	$3.60 \pm 0.13^{+0.61}_{-0.41}$	$3.44 \pm 0.13^{+0.38}_{-0.32}$	3.52 ± 0.34
BABAR/Belle untagged	$3.47 \pm 0.06^{+0.37}_{-0.32}$	$3.43 \pm 0.09^{+0.59}_{-0.39}$	$3.27 \pm 0.09^{+0.36}_{-0.30}$	3.23 ± 0.30
Belle tagged [38]	$3.38 \pm 0.17^{+0.37}_{-0.31}$	$3.86 \pm 0.25^{+0.53}_{-0.53}$	$3.69 \pm 0.24^{+0.39}_{-0.35}$	—

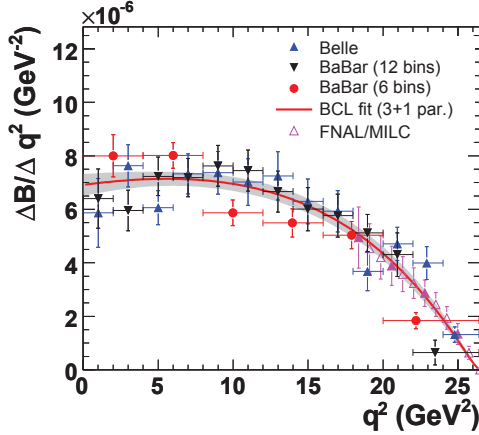


FIG. 4: Simultaneous fit of the BCL parameterization to the $\Delta\mathcal{B}/\Delta q^2$ distributions for $B \rightarrow \pi \ell \nu$ decays and to four of the twelve points of the FNAL/MILC calculation (magenta, closed triangles). The FNAL/MILC prediction has been rescaled to the data according to the $|V_{ub}|$ value obtained in the fit.

SF cannot be calculated from first principles, but has to be constrained by data. SF parameterizations are generally chosen such that their first and second moments are equal to $\overline{\Lambda} = m_B - m_b$ and μ_π^2 , i.e., they are directly related to the non-perturbative HQE parameters and thus can be determined by fits to moments of $B \rightarrow X_c \ell \nu$ and $B \rightarrow X_s \gamma$ decays.

The extracted values of $|V_{ub}|$ are presented in Table IV for both untagged and tagged $B\overline{B}$ samples. The earlier untagged measurements placed cuts near the kinematic limit of the lepton spectrum. Thus they covered limited fractions of the total phase space and had sizable experimental and theoretical uncertainties. The most recent analyses by the Belle [46] and BABAR [42] Collaborations are based on their full data

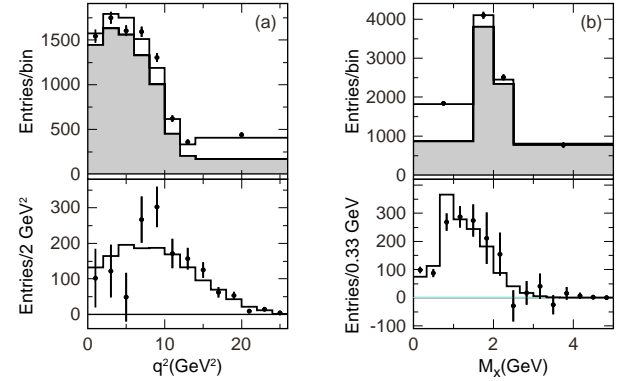


FIG. 5: BABAR [42]: Projections of measured distributions (data points) of (a) q^2 and (b) M_X for inclusive $B \rightarrow X_u \ell \nu$ decays. Upper row: comparison with the result of a χ^2 fit to the two-dimensional $M_X - q^2$ distribution for the sum of two scaled MC contributions, signal (white) and background (grey). Lower row: corresponding spectra with equal bin size after background subtraction based on the fit. The data are not efficiency corrected.

sample and use $B\overline{B}$ events tagged by the hadronic decays of the second B meson and thus cover up to 90% of the phase space. The most precise results are based on a fit to the two-dimensional q^2 versus M_X (the mass of the X_u system) distributions. An example of such a fit is shown in Figure 5. The average of the two partial branching fraction measurements, assuming full correlation of the uncertainty in the predicted signal spectrum, is $\Delta\mathcal{B}(p_\ell^* > 1 \text{ GeV}) = (1.87 \pm 0.10 \pm 0.11) \times 10^{-3}$. Here p_ℓ^* refers to the momentum of the charged lepton in the rest frame of the B meson. The systematic uncertainties are dominated by the simulation of the signal decays; in particular, they are sensitive to the shape function and the b -quark mass.

There is a high degree of consistency among the

TABLE IV: Overview of $|V_{ub}|$ measurements based on inclusive $B \rightarrow X_u \ell \nu$ decays analyzed in three untagged and 2 tagged data samples. The critical input parameters m_b and μ_π^2 depend on the different mass schemes and have been obtained from the OPE fits to $B \rightarrow X_c \ell \nu$ hadronic mass moments in the kinetic mass scheme. For the BLNP and DGE calculations, they have been translated from the kinetic to the shape function and \overline{MS} schemes, respectively. The additional uncertainties on m_b and μ_π^2 are due to these scheme translations. The first error is the experimental and the second reflects the uncertainties of the QCD calculations and the HQE parameters [3].

	BLNP	GGOU	DGE
Mass scheme	SF scheme	Kinetic scheme	\overline{MS} scheme
m_b (GeV)	$4.588 \pm 0.023 \pm 0.011$	4.560 ± 0.023	4.194 ± 0.043
μ_π^2 (GeV ²)	$0.189^{+0.041}_{-0.040} \pm 0.020$	0.453 ± 0.036	—
Experiment	$ V_{ub} $ (10^{-3})		
Belle [43]	$4.88 \pm 0.45^{+0.24}_{-0.27}$	$4.75 \pm 0.44^{+0.17}_{-0.22}$	$4.79 \pm 0.44^{+0.21}_{-0.24}$
BABAR[44]	$4.48 \pm 0.25^{+0.27}_{-0.28}$	$4.29 \pm 0.24^{+0.18}_{-0.24}$	$4.28 \pm 0.24^{+0.22}_{-0.24}$
BABAR[45]	$4.66 \pm 0.31^{+0.31}_{-0.36}$	—	$4.32 \pm 0.29^{+0.24}_{-0.29}$
Average untagged	$4.65 \pm 0.22^{+0.26}_{-0.29}$	$4.39 \pm 0.22^{+0.18}_{-0.24}$	$4.44 \pm 0.21^{+0.21}_{-0.25}$
Belle [46]	$4.47 \pm 0.27^{+0.19}_{-0.21}$	$4.54 \pm 0.27^{+0.10}_{-0.11}$	$4.60 \pm 0.27^{+0.11}_{-0.13}$
BABAR[42]	$4.28 \pm 0.24^{+0.18}_{-0.20}$	$4.35 \pm 0.24^{+0.09}_{-0.11}$	$4.40 \pm 0.24^{+0.12}_{-0.13}$
Average tagged	$4.35 \pm 0.19^{+0.19}_{-0.20}$	$4.43 \pm 0.21^{+0.09}_{-0.11}$	$4.49 \pm 0.21^{+0.13}_{-0.13}$

measurements and the results for different QCD calculations show little variation. Based on results in Table IV, we quote the unweighted arithmetic average of the tagged data samples as the overall result,

$$|V_{ub}|_{\text{incl}} = (4.42 \pm 0.20_{\text{exp}} \pm 0.15_{\text{th}}) \times 10^{-3}. \quad (7)$$

E. Summary on $|V_{cb}|$ and $|V_{ub}|$

As a result of joint efforts by theorists and experimentalists, our understanding of semileptonic B -meson decays has substantially advanced over the last decade.

Substantial progress has been made in the application of HQE calculations to extract $|V_{cb}|$ and m_b from fits to measured moments from $B \rightarrow X_c \ell \nu$ decays. The total error quoted on $|V_{cb}|$ is 1.8% and the introduction of a c -quark mass constraint, $m_c(3 \text{ GeV}) = (0.998 \pm 0.029) \text{ GeV}$, has reduced the overall uncertainty on m_b to 25 MeV.

The measurement of $|V_{cb}|$ based on the exclusive decay $B \rightarrow D^* \ell \nu_\ell$ has now a combined experimental and theoretical uncertainty of 2.3%. Values of $|V_{cb}|$ differ by about 5%, depending on the choice of the QCD calculation for the normalization of the form factors; lattice calculations lead to lower values of $|V_{cb}|$ than heavy flavor sum rules.

Consequently the comparison of the inclusive and exclusive determinations of $|V_{cb}|$ depends on the choice of the normalization of the form factors. For the LQCD calculations, the values of the inclusive and exclusive determination of $|V_{cb}|$ differ at the level of

2.5σ ,

$$\begin{aligned} |V_{cb}|_{\text{excl}} &= [39.04 (1 \pm 0.014_{\text{exp}} \pm 0.019_{\text{th}})] \times 10^{-3}, \\ |V_{cb}|_{\text{incl}} &= [42.01 (1 \pm 0.011_{\text{exp}} \pm 0.014_{\text{th}})] \times 10^{-3}. \end{aligned}$$

On the other hand, based on heavy flavor sum rule calculations for the exclusive measurement, the value is

$$|V_{cb}|_{\text{excl}} = [40.93 (1 \pm 0.014_{\text{exp}} \pm 0.023_{\text{th}})] \times 10^{-3}$$

and agrees very well with the inclusive measurement.

For inclusive measurements of $|V_{ub}|$, experimental and theoretical errors are comparable in size. The dominant experimental uncertainties are related to the limited size of the tagged samples, the signal simulation, and background subtraction. The theoretical uncertainties are dominated by the error on the b -quark mass; a 20-30 MeV uncertainty in m_b impacts $|V_{ub}|$ by 2-3%.

Measurements of the differential decay rate as a function of q^2 for $B \rightarrow \pi \ell \nu$ provide valuable information on the shape of the form factor, though with sizable errors due to large backgrounds. Results based on different QCD calculations agree within the stated theoretical uncertainties. While the traditional method of normalizing to QCD calculations in different ranges of q^2 results in uncertainties of $^{+17\%}_{-10\%}$, combined fits to LQCD predictions and the measured spectrum using a theoretically motivated ansatz [32–34] have resulted in a reduction of the theoretical uncertainties to about 8%.

The values of the inclusive and exclusive determinations of $|V_{ub}|$ are only marginally consistent, they differ at a level of 3σ ,

$$\begin{aligned} |V_{ub}|_{\text{excl}} &= [3.23 (1 \pm 0.05_{\text{exp}} \pm 0.08_{\text{th}})] \times 10^{-3} \\ |V_{ub}|_{\text{incl}} &= [4.42 (1 \pm 0.045_{\text{exp}} \pm 0.034_{\text{th}})] \times 10^{-3}. \end{aligned}$$

III. STUDY OF $\bar{B} \rightarrow D^{(*)}\tau^-\bar{\nu}_\tau$ DECAYS

So far, we have focused on semileptonic decays involving low-mass charged leptons, for instance, $\bar{B} \rightarrow D^{(*)}\ell^-\bar{\nu}_\ell$ decays which are well-understood SM processes. Decays involving the higher mass τ lepton provide an opportunity to search for contributions beyond the SM processes, for example, decays mediated by a charged Higgs boson of the Two Higgs Doublet Model (2HDM) of type II [47–52].

In the SM, the differential decay rate (integrated over angles) for $\bar{B} \rightarrow D^{(*)}\tau^-\bar{\nu}_\tau$ decays can be written in terms of helicity amplitudes as follows [53–55],

$$\frac{d\Gamma_\tau}{dq^2} = \frac{G_F^2 |V_{cb}|^2 |\mathbf{p}| q^2}{96\pi^3 m_B^2} \left[1 - \frac{m_\tau^2}{q^2} \right]^2 \left([|H_+|^2 + |H_-|^2 + |H_0|^2] \left[1 + \frac{m_\tau^2}{2q^2} \right] + \frac{3}{2} \frac{m_\tau^2}{q^2} |H_s|^2 \right), \quad (8)$$

where for simplicity, the q^2 dependence of the helicity amplitudes H_n has been omitted. The amplitudes H_\pm only receive contributions from helicity $\lambda_{D^*} = \pm$ and therefore are absent for $\bar{B} \rightarrow D\tau^-\bar{\nu}_\tau$ decays. $\lambda_{D^*} = 0$ contribute to H_0 and H_s . SM calculations [52, 56], updated to account for recent FF measurements, predict for the ratios of decay rates,

$$\mathcal{R}(D)_{\text{SM}} = \frac{\Gamma(\bar{B} \rightarrow D\tau\nu)}{\Gamma(\bar{B} \rightarrow D\ell\nu)} = 0.297 \pm 0.017,$$

$$\mathcal{R}(D^*)_{\text{SM}} = \frac{\Gamma(\bar{B} \rightarrow D^*\tau\nu)}{\Gamma(\bar{B} \rightarrow D^*\ell\nu)} = 0.252 \pm 0.003.$$

These ratios are independent of $|V_{cb}|$ and to a large extent, insensitive to the parameterization of the hadronic matrix element. Previous measurements [57–59] have slightly exceeded these predictions, though due to sizable statistical uncertainties the significance of the measured excess was low.

The BABAR Collaboration reports results [60] of a major update of its earlier measurement [58] of the ratios $\mathcal{R}(D^{(*)})$ for both charged and neutral B mesons. They choose to reconstruct only the leptonic decays $\tau^- \rightarrow \ell^-\bar{\nu}_\ell\nu_\tau$, so that the final states of the signal $\bar{B} \rightarrow D^{(*)}\tau^-\bar{\nu}_\tau$ and the normalization $\bar{B} \rightarrow D^{(*)}\ell^-\bar{\nu}_\ell$ decays contain the same particles, *i.e.*, a charm meson $D^{(*)}$ and a charged lepton, e^- or μ^- . This leads to a cancelation of various experimental uncertainties in the ratios $\mathcal{R}(D^{(*)})$.

The analysis relies on the reconstruction of the full $B\bar{B}$ final state. In addition to the semileptonic decay, the hadronic decay of the other B meson is fully reconstructed. Compared to the previous BABAR analysis [58], the efficiency of the B tagging algorithm and the reconstruction of the semileptonic decays has been increased by a factor of three, and the size of the data sample is doubled.

The events are divided into four subsamples identified by the charm meson from a semileptonic decay candidate, $D^0\ell, D^{*0}\ell, D^+\ell, D^{*+}\ell$. The missing mass $m_{\text{miss}}^2 = (p_{e^+e^-} - p_{\text{tag}} - p_{D^{(*)}} - p_\ell)^2$ separates the normalization decays with $m_{\text{miss}}^2 \sim 0$ (one neutrino) from signal decays with much larger m_{miss}^2 (three neutrinos). The leptons in normalization decays have higher momenta than the secondary leptons from τ decays, and this feature is also utilized to separate the two decay modes. Decays to higher-mass, excited charm mesons, $B \rightarrow D^{**}\ell/\tau\nu$, enter the event selection, whenever the low momentum pion from $D^{**} \rightarrow D^{(*)}\pi$ decays is undetected or incorrectly assigned to the B_{tag} . These higher-mass states are poorly understood and their branching fractions are not well measured. Therefore the fit includes four control $D^{(*)}\pi^0\ell$ samples, enriched in $B \rightarrow D^{**}\ell/\tau\nu$ decays, by adding a π^0 decay to the signal selection.

The background in these 8 samples is reduced by applying multivariate methods (BDT) that make use of variables describing the quality of the reconstruction, such as the mass of the reconstructed $D^{(*)}$ and $\Delta E = E_{\text{tag}} - \sqrt{s}/2$, where E_{tag} and \sqrt{s} refer to the B_{tag} and the center of mass energy, respectively. Candidates with one or more additional charged tracks are eliminated. The yields for semileptonic decay of the four signal $\bar{B} \rightarrow D^{(*)}\tau^-\bar{\nu}_\tau$ decays and four normalization $\bar{B} \rightarrow D^{(*)}\ell^-\bar{\nu}_\ell$ decays are extracted by an extended, unbinned maximum-likelihood fit to the two-dimensional m_{miss}^2 versus $|\mathbf{p}_\ell^*|$ distributions. The fit is performed simultaneously to the four $D^{(*)}\ell$ samples and the four $D^{(*)}\pi^0\ell$ samples. The distribution of each $D^{(*)}\ell$ sample is described as the sum of eight contributions: $D\tau\nu, D^*\tau\nu, D\ell\nu, D^*\ell\nu, D^{**}\ell\nu$, cross-feed between B^0 and B^+ due to misreconstruction of the B_{tag} , and backgrounds from $B\bar{B}$ and continuum events. The yields and shapes of these backgrounds are taken from MC simulation and fixed in the fit. A large fraction of $B \rightarrow D^*\ell\nu$ decays are reconstructed in the $D\ell\nu$ samples. A total of 56 two-dimensional probability density functions (PDF) for the individual contributions to the samples are constructed from large Monte Carlo samples by using Gaussian Kernel Estimators (KEYS). The fitted distributions for $D\ell$ and $D^*\ell$ samples are shown in Figure 6. The results for charged and neutral B mesons are combined, assuming isospin relations. In total, there are 489 ± 63 $\bar{B} \rightarrow D\tau^-\bar{\nu}_\tau$ compared to $2,981 \pm 65$ $\bar{B} \rightarrow D\ell^-\bar{\nu}_\ell$ decays, and 888 ± 63 $\bar{B} \rightarrow D^*\tau^-\bar{\nu}_\tau$ compared to $11,953 \pm 122$ $\bar{B} \rightarrow D^*\ell^-\bar{\nu}_\ell$ decays.

The measured ratios, corrected for efficiencies and branching fractions, are

$$\mathcal{R}(D) = 0.440 \pm 0.058 \pm 0.042,$$

$$\mathcal{R}(D^*) = 0.332 \pm 0.024 \pm 0.017.$$

The principal contributions to the systematic errors are the uncertainties in the $B \rightarrow D^{**}\ell/\tau\nu$ and continuum backgrounds and the limited size of the MC

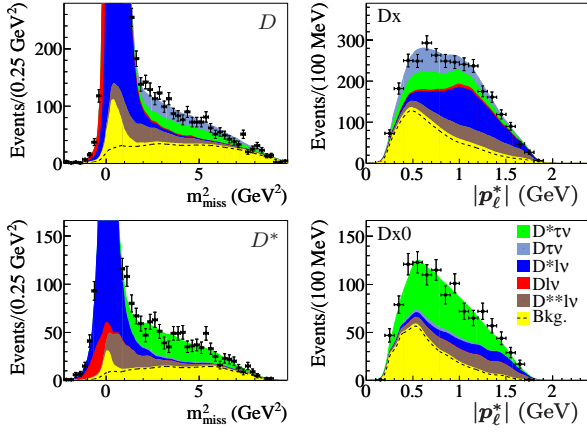


FIG. 6: m^2_{miss} and $|\mathbf{p}^*_\ell|$ projections of the isospin-constrained fit to the signal samples. The $|\mathbf{p}^*_\ell|$ projections do not include the m^2_{miss} peak at $m^2_{\text{miss}} < 1 \text{ GeV}^2$, which excludes most of the normalization events [60].

samples. The measurements exceed the SM calculations by 2.0σ and 2.7σ . The combination of these results, taking into account their correlation of -0.27 , excludes the SM at the 3.4σ level.

The charged Higgs boson H^+ would only impact the helicity amplitude H_s ,

$$H_s^{\text{2HDM}} = H_s^{\text{SM}} \left[1 - \frac{m_b q^2}{m_b \mp m_c} \frac{\tan^2 \beta}{m_H^2} \right]. \quad (9)$$

The negative sign applies to $\bar{B} \rightarrow D\tau^-\bar{\nu}_\tau$ and the positive sign to $\bar{B} \rightarrow D^*\tau^-\bar{\nu}_\tau$ decays. Depending on the value of $\tan\beta/m_{H^+}$, the ratio of two vacuum expectations values and the mass of the charged Higgs, this term would either enhance or decrease the ratios $\mathcal{R}(D^{(*)})$ and affect the τ polarization.

Figure 7 shows the impact a charged 2HDM type II Higgs boson [51, 61] would have on the measured ratios $\mathcal{R}(D)$ and $\mathcal{R}(D^*)$ as a function $\tan\beta/m_{H^+}$. This assessment was made by reweighting the simulated events to account for the changes in the matrix element, including the τ polarization.

The measured values of $\mathcal{R}(D)$ and $\mathcal{R}(D^*)$ match the predictions of this particular Higgs model for $\tan\beta/m_{H^+} = (0.44 \pm 0.02) \text{ GeV}^{-1}$ and $\tan\beta/m_{H^+} = (0.75 \pm 0.04) \text{ GeV}^{-1}$, respectively. The $\mathcal{R}(D)$ and $\mathcal{R}(D^*)$ results together exclude the type II 2HDM charged Higgs boson at at 99.8% confidence level, or higher for larger values of $\tan\beta/m_{H^+}$. This conclusion is only valid for values of m_{H^+} greater than 15 GeV [48, 51]. However, the region for $m_{H^+} \leq 15 \text{ GeV}$ has already been excluded by $B \rightarrow X_s \gamma$ measurements [62], and therefore, the type II 2HDM is excluded in the full $\tan\beta$ - m_{H^+} parameter space.

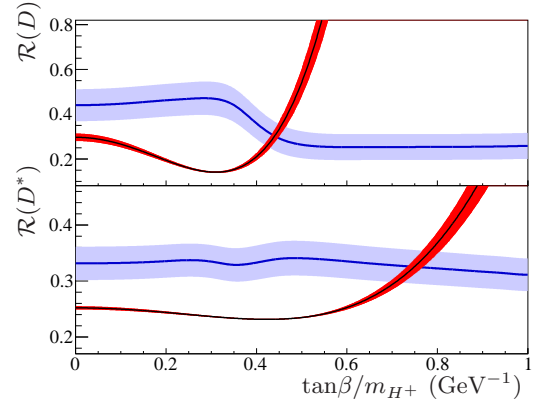


FIG. 7: Comparison of the results of the *BABAR* analysis (light grey, blue) [60] with predictions that include a charged Higgs boson of type II 2HDM (dark grey, red). The SM corresponds to $\tan\beta/m_{H^+} = 0$.

IV. CONCLUSIONS AND OUTLOOK

While there has been tremendous progress, we have not achieved the precision of 1% for $|V_{cb}|$ or 5% on $|V_{ub}|$, goals many of us had hoped to reach before the shutdown of Belle and *BABAR* experiments.

We are left with two puzzles:

- The puzzling difference, in the results of exclusive and inclusive measurements of $|V_{ub}|$ and to lesser extent of $|V_{cb}|$, if we rely on non-lattice calculations, which challenge our current understanding of the experimental and theoretical techniques applied.
- The excess of events in $\bar{B} \rightarrow D^{(*)}\tau^-\bar{\nu}_\tau$ decays at the level of 3.4 standard deviations relative to the SM calculations, which might indicate non-SM contributions. This excess cannot be explained by contributions from a charged Higgs boson of the 2HDM of type II. However, it has been pointed out in recent publications [63, 64] that this result can be accommodated in terms of other versions of the Two-Higgs Doublet Model.

To resolve these puzzles a major effort will be required. It will take much larger tagged data samples and a more detailed understanding of the detector performance and background composition to reduce experimental uncertainties. It will also require further progress in QCD calculations, based on lattice, heavy flavor sum rules, or other methods, to reduce the uncertainties of form factor predictions for exclusive decays, to improve the detailed prediction of inclusive processes, and to incorporate precision determinations of the heavy quark masses.

Measurements of the D^* and τ polarization and forward-backward asymmetries as well as other kinematic distributions might be able to distinguish

among various couplings of non-SM processes [65, 66] and possibly lead to an explanation of the excess events in $\bar{B} \rightarrow D^{(*)}\tau^-\bar{\nu}_\tau$ decays.

Acknowledgments

The author would like to thank the organizers of FPCP 2012, in particular Zheng-guo Zhao and his colleagues at USTC in Hefei for a very exciting conference. The summary of the results on $|V_{cb}|$ and $|V_{ub}|$

is heavily based on the *Physics of the B Factories*, a book that has been assembled by the BABAR and Belle Collaborations with the support of many theorists. I consider myself privileged to have been part of this effort. Last not least, I would like to acknowledge the contributions of Manuel Franco Sevilla, who recently completed his PhD thesis on the $\bar{B} \rightarrow D^{(*)}\tau^-\bar{\nu}_\tau$ decays and the observation of an excess of events above Standard Model expectations.

This work was supported by Department of Energy contract DE-AC03-76SF00515.

-
- [1] Throughout this report, charge-conjugate decay modes are implied.
 - [2] *Physics of the B Factories (in preparation)* (2012).
 - [3] Y. Amhis et al. (Heavy Flavor Averaging Group) (2012), hep-ex/1207.1158.
 - [4] A. Sirlin, Nucl. Phys. **B196**, 83 (1982).
 - [5] I. Caprini, L. Lellouch, and M. Neubert, Nucl. Phys. **B530**, 153 (1998), hep-ph/9712417.
 - [6] B. Aubert et al. (BABAR Collaboration), Phys.Rev.Lett. **104**, 011802 (2010), hep-ex/0904.4063.
 - [7] B. Aubert et al. (BABAR), Phys. Rev. **D77**, 032002 (2008), hep-ex/0705.4008.
 - [8] W. Dungel et al. (Belle Collaboration), Phys.Rev. **D82**, 112007 (2010), hep-ex/1010.5620.
 - [9] B. Aubert et al. (BABAR Collaboration), Phys.Rev. **D74**, 092004 (2006), hep-ex/0602023.
 - [10] J. Beringer et al. (Particle Data Group), Phys.Rev. **D86**, 010001 (2012).
 - [11] K. Abe et al. (Belle Collaboration), Phys.Lett. **B526**, 258 (2002), hep-ex/0111082.
 - [12] B. Aubert et al. (BABAR Collaboration), Phys.Rev. **D79**, 012002 (2009), hep-ex/0809.0828.
 - [13] B. Aubert et al. (BABAR Collaboration), Phys.Rev.Lett. **100**, 231803 (2008), hep-ex/0712.3493.
 - [14] M. Okamoto, C. Aubin, C. Bernard, C. E. DeTar, M. Di Pierro, et al., Nucl.Phys.Proc.Suppl. **140**, 461 (2005), hep-lat/0409116.
 - [15] N. Uraltsev, Phys.Lett. **B585**, 253 (2004), hep-ph/0312001.
 - [16] C. Bernard et al. (Fermilab Lattice and MILC Collaborations), Phys. Rev. **D79**, 014506 (2009), hep-lat/0808.2519.
 - [17] J. A. Bailey et al. (Fermilab Lattice and MILC Collaborations), PoS **LATTICE2010**, 311 (2010), hep-lat/1011.2166.
 - [18] P. Gambino, T. Mannel, and N. Uraltsev, Phys. Rev. **D81**, 113002 (2010), hep-ph/1004.2859.
 - [19] A. H. Hoang, Z. Ligeti, and A. V. Manohar, Phys.Rev. **D59**, 074017 (1999), hep-ph/9811239.
 - [20] C. W. Bauer, Z. Ligeti, M. Luke, A. V. Manohar, and M. Trott, Phys.Rev. **D70**, 094017 (2004), hep-ph/0408002.
 - [21] I. I. Bigi, M. A. Shifman, N. Uraltsev, and A. I. Vainshtein, Phys.Rev. **D52**, 196 (1995), hep-ph/9405410.
 - [22] D. Benson, I. Bigi, T. Mannel, and N. Uraltsev, Nucl.Phys. **B665**, 367 (2003), hep-ph/0302262.
 - [23] I. I. Bigi, M. A. Shifman, N. Uraltsev, and A. I. Vainshtein, Phys.Rev. **D56**, 4017 (1997), hep-ph/9704245.
 - [24] P. Gambino, JHEP **1109**, 055 (2011), hep-ph/1107.3100.
 - [25] P. Gambino and C. Schwanda (2011), hep-ex/1102.0210.
 - [26] C. Schwanda et al. (Belle Collaboration), Phys.Rev. **D78**, 032016 (2008), hep-ex/0803.2158.
 - [27] B. Aubert et al. (BABAR Collaboration), Phys.Rev. **D81**, 032003 (2010), hep-ex/0908.0415.
 - [28] B. Dehnadi, A. H. Hoang, V. Mateu, and S. M. Zebarjad (2011), hep-ph/1102.2264.
 - [29] K. G. Chetyrkin et al., Phys. Rev. **D80**, 074010 (2009), hep-ph/0907.2110.
 - [30] C. McNeile, C. T. H. Davies, E. Follana, K. Hornbostel, and G. P. Lepage, Phys. Rev. **D82**, 034512 (2010), hep-lat/1004.4285.
 - [31] F. J. Gilman and R. L. Singleton, Phys.Rev. **D41**, 142 (1990).
 - [32] C. G. Boyd, B. Grinstein, and R. F. Lebed, Phys.Rev.Lett. **74**, 4603 (1995), hep-ph/9412324.
 - [33] T. Becher and R. J. Hill, Phys.Lett. **B633**, 61 (2006), hep-ph/0509090.
 - [34] C. Bourrely, I. Caprini, and L. Lellouch, Phys.Rev. **D79**, 013008 (2009), hep-ph/0807.2722.
 - [35] P. del Amo Sanchez et al. (BABAR Collaboration), Phys.Rev. **D83**, 032007 (2011), hep-ex/1005.3288.
 - [36] P. del Amo Sanchez et al. (BABAR Collaboration), Phys.Rev. **D83**, 052011 (2011), hep-ex/1010.0987.
 - [37] H. Ha et al. (BELLE Collaboration), Phys.Rev. **D83**, 071101 (2011), hep-ex/1012.0090.
 - [38] C. Beleno (Belle Collaboration), *Exclusive Charmless Semileptonic B Decays at Belle, presentation at Lake Louise Winter School* (2012).
 - [39] J. A. Bailey, C. Bernard, C. E. DeTar, M. Di Pierro, A. El-Khadra, et al., Phys.Rev. **D79**, 054507 (2009), hep-lat/0811.3640.
 - [40] A. Khodjamirian, T. Mannel, N. Offen, and Y.-M. Wang, Phys.Rev. **D83**, 094031 (2011), hep-ph/1103.2655.
 - [41] E. Dalgic, A. Gray, M. Wingate, C. T. Davies, G. P. Lepage, et al., Phys.Rev. **D73**, 074502 (2006), hep-lat/0601021.
 - [42] J. Lees et al. (BABAR Collaboration) (2012), hep-

- ex/1208.1253.
- [43] A. Limosani et al. (Belle Collaboration), *Phys.Lett.* **B621**, 28 (2005), hep-ex/0504046.
 - [44] B. Aubert et al. (BABAR Collaboration), *Phys.Rev.* **D73**, 012006 (2006), hep-ex/0509040.
 - [45] B. Aubert et al. (BABAR Collaboration), *Phys.Rev.Lett.* **95**, 111801 (2005), hep-ex/0506036.
 - [46] P. Urquijo et al. (Belle Collaboration), *Phys.Rev.Lett.* **104**, 021801 (2010), hep-ex/0907.0379.
 - [47] B. Grzadkowski and W.-S. Hou, *Phys. Lett. B* **283**, 427 (1992).
 - [48] M. Tanaka, *Z. Phys. C* **67**, 321 (1995).
 - [49] H. Itoh, S. Komine, and Y. Okada, *Prog. Theor. Phys.* **114**, 179 (2005), hep-ph/0409228.
 - [50] U. Nierste, S. Trine, and S. Westhoff, *Phys. Rev. D* **78**, 015006 (2008), hep-ph/0801.4938.
 - [51] M. Tanaka and R. Watanabe, *Phys. Rev. D* **82**, 034027 (2010).
 - [52] S. Fajfer, J. F. Kamenik, and I. Nisandzic, *Phys.Rev.* **D85**, 094025 (2012), hep-ph/1203.2654.
 - [53] J. G. Korner and G. A. Schuler, *Z. Phys. C* **46**, 93 (1990).
 - [54] A. F. Falk, Z. Ligeti, M. Neubert, and Y. Nir, *Phys. Lett. B* **326**, 145 (1994), hep-ph/9401226.
 - [55] D. S. Hwang and D. W. Kim, *Eur. Phys. J.* **C14**, 271 (2000).
 - [56] J. F. Kamenik and F. Mescia, *Phys. Rev. D* **78**, 014003 (2008), hep-ph/0802.3790.
 - [57] A. Matyja et al. (Belle Collaboration), *Phys. Rev. Lett.* **99**, 191807 (2007), hep-ex/0706.4429.
 - [58] B. Aubert et al. (BABAR Collaboration), *Phys. Rev. Lett.* **100**, 021801 (2008), hep-ex/0709.1698.
 - [59] A. Bozek et al. (Belle Collaboration), *Phys. Rev. D* **82**, 072005 (2010), hep-ex/1005.2302.
 - [60] J. Lees et al. (BaBar Collaboration), *Phys.Rev.Lett.* **109**, 101802 (2012), hep-ex/1205.5442.
 - [61] V. D. Barger, J. Hewett, and R. Phillips, *Phys. Rev. D* **41**, 3421 (1990).
 - [62] M. Misiak et al., *Phys. Rev. Lett.* **98**, 022002 (2007), hep-ph/0609232.
 - [63] S. Fajfer, J. F. Kamenik, I. Nisandzic, and J. Zupan (2012), hep-ph/1206.1872.
 - [64] A. Crivellin, C. Greub, and A. Kokulu (2012), hep-ph/1206.2634.
 - [65] A. Datta, M. Duraisamy, and D. Ghosh (2012), hep-ph/1206.3760.
 - [66] D. Becirevic, N. Kosnik, and A. Tayduganov, *Phys.Lett.* **B716**, 208 (2012), 1206.4977.